Two distinct mechanisms target GAD67 to vesicular pathways and presynaptic clusters

Jamil Kanaani,[1] Julia Kolibachuk,[1] Hugo Martinez,[2] and Steinunn Baekkeskov[1,3,4]

[1]Diabetes Center, [2]Department of Biochemistry and Biophysics, [3]Department of Medicine, and [4]Department of Microbiology and Immunology, University of California, San Francisco, San Francisco, CA 94143

The inhibitory neurotransmitter γ-amino butyric acid (GABA) is synthesized by two isoforms of the enzyme glutamic acid decarboxylase (GAD): GAD65 and GAD67. Whereas GAD67 is constitutively active and produces >90% of GABA in the central nervous system, GAD65 is transiently activated and augments GABA levels for rapid modulation of inhibitory neurotransmission. Hydrophobic lipid modifications of the GAD65 protein target it to Golgi membranes and synaptic vesicles in neuroendocrine cells. In contrast, the GAD67 protein remains hydrophilic but has been shown to acquire membrane association by heterodimerization with GAD65. Here, we identify a second mechanism that mediates robust membrane anchoring, axonal targeting, and presynaptic clustering of GAD67 but that is independent of GAD65. This mechanism is abolished by a leucine-103 to proline mutation that changes the conformation of the N-terminal domain but does not affect the GAD65-dependent membrane anchoring of GAD67. Thus two distinct mechanisms target the constitutively active GAD67 to presynaptic clusters to facilitate accumulation of GABA for rapid delivery into synapses.

Introduction

The distinct functions of the GAD65 and GAD67 isoforms have mainly emerged from studies of knockout mice. Ablation of *GAD67* results in >90% reduction in basal γ-amino butyric acid (GABA) levels in the brain, a cleft palate, and neonatal lethality (Asada et al., 1997; Condie et al., 1997). Conditional knockdown of *GAD67* in the brain has revealed the role of GABA, generated by this isoform, in development of neuronal circuits in the visual cortex (Chattopadhyaya et al., 2007). In contrast, GABA synthesized by GAD65 is not required for development and early survival but is critical for fast modulation of inhibitory neurotransmission in response to an increase in demand. Thus, GAD65$^{-/-}$ mice show no obvious developmental abnormalities but are prone to epileptic seizures (Asada et al., 1996; Kash et al., 1997) and increased anxiety (Kash et al., 1999), and have defects in handling of environmental stimuli, including light and stress (Hensch et al., 1998; Stork et al., 2000, 2003; Shimura et al., 2004). The evidence from GAD67$^{-/-}$ and GAD65$^{-/-}$ mice is consistent with GAD67 providing the magnitude of basal firing of GABA for inhibitory neurotransmission, whereas transiently activated GAD65 synthesizes GABA for high-frequency bursts to fine-tune GABAergic synaptic function (Tian et al., 1999; Patel et al., 2006).

The *GAD67* and *GAD65* genes are derived from a common precursor and share extensive homology in the middle and C-terminal domains. However, they differ significantly in the N-terminal region, with only 22% identity in exons 1–3 (aa 1–95 in GAD65 and 1–101 in GAD67; Bu et al., 1992). The crystal structure of N-terminal truncations of GAD67 and GAD65 has revealed extensive similarities in the three-dimensional structure of the middle and C-terminal domains (aa 84–585 in GAD65, 90–593 in GAD67; Fenalti et al., 2007). There is, however, a striking difference in the structure of the catalytic loop of the two isoforms (Fenalti et al., 2007), which is consistent with a stable binding of the coenzyme pyridoxal 5′-phosphate (PLP) to GAD67, whereas GAD65 oscillates between an inactive apoenzyme and an active holoenzyme (Battaglioli et al., 2003). The diverse N-terminal regions of GAD65 and GAD67 share no homology with known proteins, and the crystal structures are not available. In GAD65, the N-terminal region harbors three trafficking signals that mediate targeting to

Correspondence to Steinunn Baekkeskov: sbaekkeskov@ucsf.edu

Abbreviations used in this paper: GABA, γ-amino butyric acid; GAD, glutamic acid decarboxylase; GM130, Golgi matrix protein of 130 kD; PLP, pyridoxal 5′-phosphate; wt, wild type.

The Rockefeller University Press $30.00
J. Cell Biol. Vol. 190 No. 5 911–925
www.jcb.org/cgi/doi/10.1083/jcb.200912101

Golgi membranes and post-Golgi trafficking to cytosolic vesicles in nonneuronal cells and synaptic vesicles in neuroendocrine cells (Kanaani et al., 2002). Both GAD67 and GAD65 are synthesized as soluble hydrophilic molecules. GAD65 undergoes a series of posttranslational hydrophobic modifications in the N-terminal domain, including palmitoylation of cysteines 30 and 45 (Christgau et al., 1991, 1992; Shi et al., 1994). In contrast, GAD67 remains hydrophilic (Christgau et al., 1991, 1992; Solimena et al., 1993, 1994; Kanaani et al., 1999). After the first hydrophobic modification, GAD65 is targeted to the cytosolic face of the ER and Golgi compartments, where it cycles on and off membranes until palmitoylation in Golgi membranes results in trafficking to the TGN and post-Golgi targeting to cytosolic vesicles in nonneuronal cells (Kanaani et al., 2008). In primary neurons, GAD65 is selectively targeted to axons and presynaptic clusters. Targeting of GAD65 to synaptic vesicles circumvents the long distance between the soma and axon termini and facilitates rapid filling of synaptic vesicles to sustain intense firing of GABAergic neurons. A dynamic palmitoylation/depalmitoylation cycle continuously shuttles GAD65 between Golgi membranes and presynaptic clusters, revealing a sophisticated mechanism for rapid regulation of the levels of enzyme and its product in presynaptic membranes (Kanaani et al., 2008; for review see Baekkeskov and Kanaani, 2009). The subcellular localization of the GAD67 isoform has remained ambiguous. Recombinant rat GAD67 was soluble in transfected CHO and COS-7 cells (Solimena et al., 1993; Dirkx et al., 1995) but was shown to acquire membrane association by heterodimerization with GAD65 (Dirkx et al., 1995; Kanaani et al., 1999). However, subcellular fractionation of brains and confocal analyses of neurons from GAD65$^{-/-}$ mice showed that mouse GAD67 is firmly membrane anchored and targets to presynaptic clusters in the absence of GAD65 and in spite of lacking intrinsic hydrophobicity (Kanaani et al., 1999; Obata et al., 1999). In this study, we have analyzed the subcellular localization and membrane anchoring of endogenous rat GAD67 and of transfected recombinant rat, mouse, and human GAD67 in neurons and nonneuronal cells. The studies reveal that in all three species, GAD67 is targeted to membranes and vesicular trafficking pathways independent of GAD65. The results suggest that in addition to membrane anchoring by heterodimerization with GAD65, which involves the middle- and C-terminal regions of the protein, a separate and similarly robust membrane-targeting mechanism, involving the N-terminal region, has evolved for GAD67 in neurons and several other cell types. This distinct mechanism mediates selective axonal targeting and presynaptic clustering of GAD67, resulting in targeting similar to that of the smaller isoform GAD65, yet independent of it.

Results

In primary neurons, GAD67 is targeted to Golgi membranes, cytosolic vesicles, and presynaptic clusters independent of GAD65

We sought to clarify the contrasting reports on the membrane anchoring properties of GAD67 and the role of GAD65 in its targeting. We first analyzed the subcellular localization of endogenous rat GAD67 in primary hippocampal neurons. Endogenous rat GAD67 and GAD65 were immunolabeled with the K2 rabbit antibody and the GAD6 monoclonal antibody, respectively. These antibodies were shown to be specific for each isoform in immunofluorescence experiments (Fig. S1). Confocal immunofluorescence analyses revealed that endogenous GAD67 in rat neurons was localized primarily in the Golgi compartment and in puncta in axons, where it showed a complete colocalization with endogenous GAD65. These GAD67/GAD65-positive puncta were also positive for the synaptic vesicle marker synaptophysin and were therefore identified as presynaptic clusters (Fig. 1). The mean total number of GAD67 containing presynaptic clusters was 211.80 ± 5.39 per neuron (mean ± SE; $n = 4$), which was the same as the number obtained for rat GAD65. This is similar to the number obtained for rat GAD65 in neuronal cultures of similar density in an earlier study (Kanaani et al., 2002). GAD67 and GAD65 also localized to similar domains in the Golgi compartment (unpublished data). Because GAD67 is coexpressed with GAD65 in GABAergic neurons, these experiments did not reveal whether GAD65 is critical for membrane anchoring of GAD67. To assess whether GAD67-GFP can be targeted to Golgi and presynaptic membranes in neurons independent of GAD65, primary rat hippocampal neurons were singly transfected with mouse, rat, or human GAD67-GFP and immunolabeled for endogenous GAD65 (with the GAD65-specific human monoclonal antibodies MICA2, -3, and -6), GFP, and for either the Golgi marker Golgi matrix protein of 130 kD (GM130) or synaptophysin. Because only 5–10% of neurons in primary hippocampal cultures are GABAergic, the majority of transfected neurons are non-GABAergic and devoid of endogenous GAD65. Confocal analyses of these experiments showed that recombinant mouse and human GAD67-GFP are targeted to Golgi membranes, somatic vesicles, and presynaptic clusters in nerve terminals in neurons that lack endogenous GAD65 (non-GABA ergic neurons, negative for GAD65; Figs. 2 and 3).

Quantitative analyses of GAD65-negative neurons transfected with GAD67-GFP revealed a mean total number of presynaptic clusters of 206.2 ± 10.9 (mean ± SE; $n = 7$) per neuron for the mouse GAD67-GFP protein and 211.2 ± 7.9 (mean ± SE; $n = 5$) per neuron for the human GAD67-GFP protein, respectively, which is similar to the number of presynaptic clusters positive for endogenous GAD67 in GABAergic rat neurons expressing GAD65 (see above in this paragraph). Thus, the absence of GAD65 in transfected neurons did not seem to negatively impact the number of presynaptic clusters targeted by GAD67-GFP. Similar transfection experiments using a recombinant rat GAD67-GFP clone were, however, dichotomous. This protein was diffuse in the soma, dendrites, and axons, and failed to associate with membrane compartments in the absence of endogenous GAD65 (Fig. 4 A). Sequencing of all three GAD65-GFP cDNA constructs revealed a nucleotide difference in the rat GAD67-GFP cDNA and in the original Bluescript clone it was derived from that had resulted in a proline in position 102 instead of the original leucine, and a second nucleotide difference resulting in leucine in position 473 instead of a valine. No changes from published sequences were found in mouse and

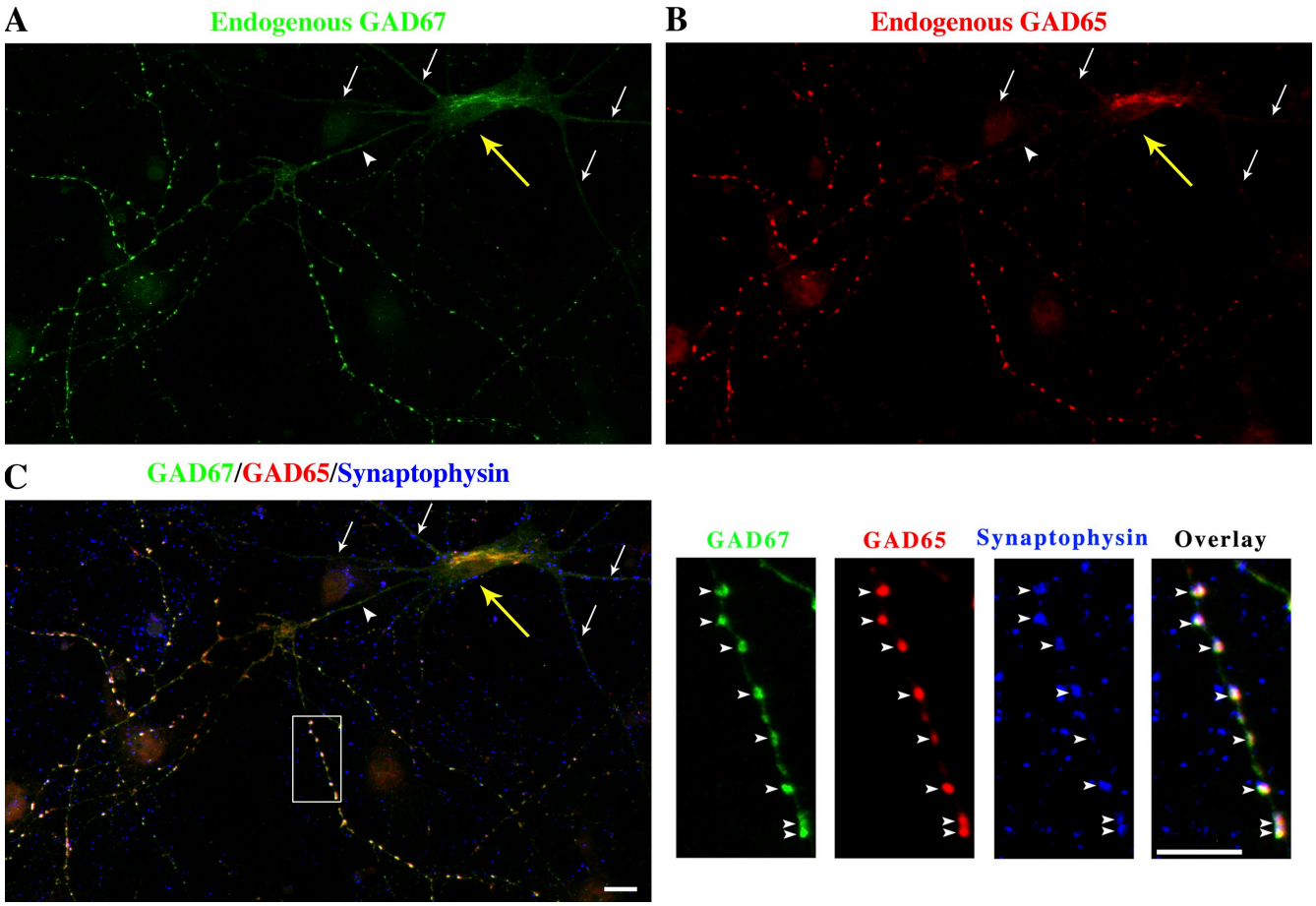

Figure 1. **Endogenous rat GAD67 is targeted to Golgi membranes and presynaptic clusters and excluded from dendrites in hippocampal neurons.** Confocal immunofluorescence analysis of endogenous GAD67, GAD65, and synaptophysin in cultured rat hippocampal neurons at day in vitro 10. The field of view has many different neurons but only one (yellow arrow) is GABAergic and shows colocalization of endogenous GAD67 (A, green) and endogenous GAD65 (B, red) in the perinuclear compartment, and with GAD65 and synaptophysin (C, blue) in presynaptic clusters in the axon (arrowheads). Merging of the triple fluorescent signals results in a white color in presynaptic clusters of the GABAergic neuron (C). GAD65 and GAD67 were not detected in the dendrites of the GABAergic neuron (arrows). Panels on the right in C show enlarged views of the boxed region. Bars, 10 μm.

human GAD67-GFP. Although the first change in rat GAD67 would be expected to have a significant effect on the conformation of the protein, the second change would be expected to have little or no effect. Consistent with this notion, engineered wild-type (wt) rat cDNA generated by reinstating leucine in position 102 and valine in position 473, as well as a version that had the wt leucine reinstated in position 102 but maintained the mutant leucine in position 473 (rat GAD67(V473L)-GFP), were indistinguishable in their membrane anchoring properties from the mouse and human GAD67 cDNAs (unpublished data). In Fig. 4 B and in the remainder of the manuscript, the reengineered cDNA clone, with amino acids 102 and 473 both reversed to the authentic rat GAD67 sequence, is referred to as wt rat GAD67. Wt rat GAD67-GFP was similar to mouse and human GAD67-GFP and targeted to Golgi membranes, cytosolic vesicles, and presynaptic clusters in axon termini lacking endogenous GAD65 (Fig. 4 B). In quantitative analysis of neurons expressing wt rat GAD67-GFP, the mean total number of presynaptic clusters containing the protein was 196.8 ± 5.4 (mean ± SE; n = 7) per neuron, whereas the number of clusters expressing rat GAD67(L102P, V473L)-GFP in neurons transfected with the corresponding construct was 9.6-fold lower (Fig. 4 C). The results show that primary neurons possess a membrane anchoring machinery that targets mouse, rat, and human GAD67 to Golgi membranes and somatic vesicles in primary neurons and mediates robust axonal targeting and presynaptic clustering independent of GAD65, yet at an efficiency similar to that obtained for GAD67 in the presence of GAD65 and for GAD65 itself. The data are consistent with the results obtained in GAD65$^{-/-}$ mice, where endogenous mouse GAD67 was shown to be firmly membrane anchored and targeted to presynaptic clusters in the absence of GAD65 (Kanaani et al., 1999; Obata et al., 1999).

Mutation of leucine 102/103 to proline in GAD67 abolishes GAD65-independent membrane anchoring of GAD67 in primary neurons, without affecting its GAD65-dependent membrane anchoring and subcellular targeting

The results described in the previous paragraph suggested that a mutation of leucine 102 to proline abolishes the ability of rat GAD67 to become membrane-anchored independent of GAD65. Leucine 102 in rat and mouse GAD67 is equivalent to leucine 103 in human GAD67. To further analyze the effect of

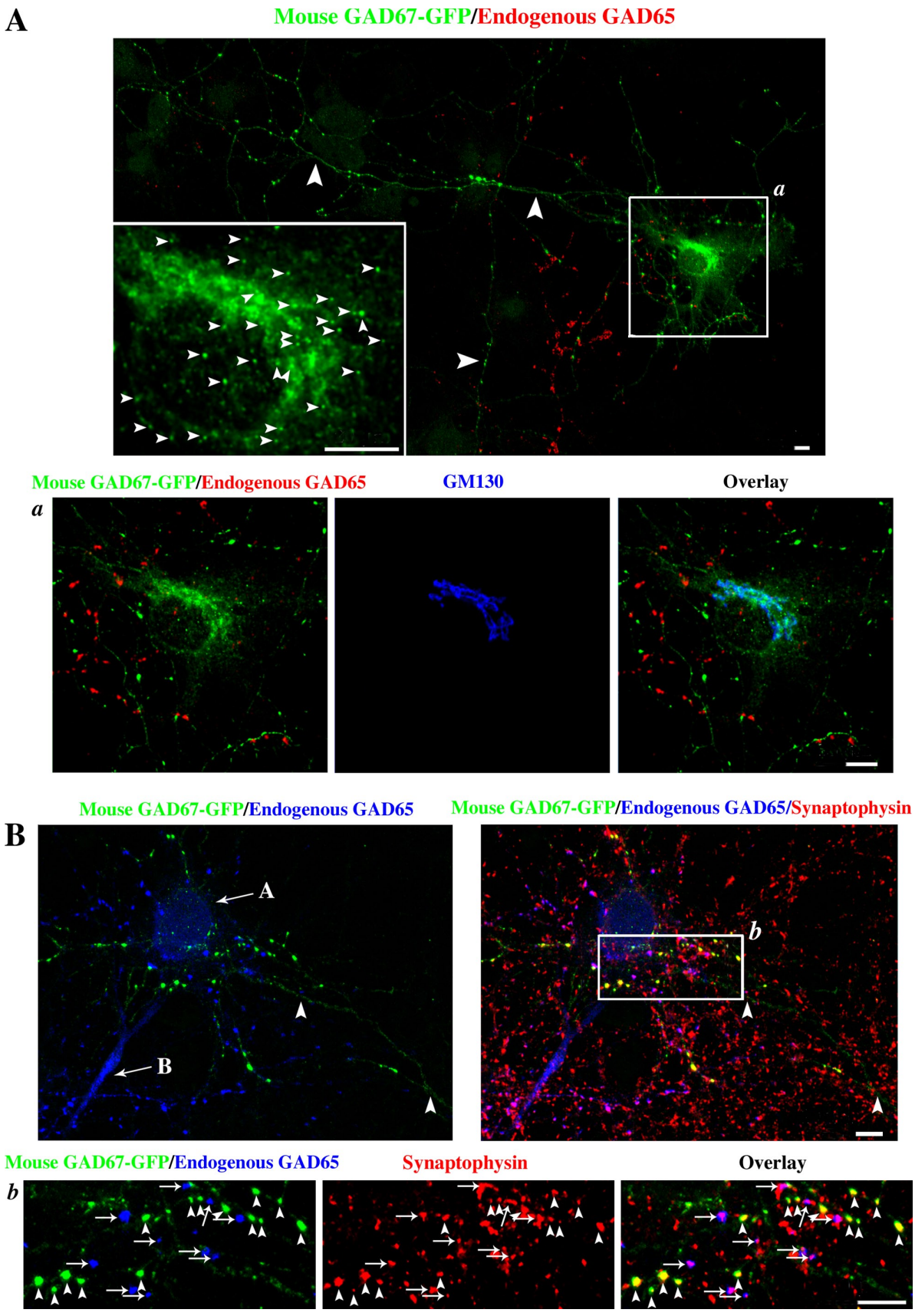

Figure 2. **Mouse GAD67-GFP is targeted to Golgi membranes, cytosolic vesicles, and presynaptic clusters in hippocampal neurons independent of endogenous GAD65.** (A) Confocal images of a rat hippocampal neuron singly transfected with mouse GAD67-GFP and triple immunolabeled for GFP (green), endogenous GAD65 (red; mixture of human monoclonal antibodies MICA 2, 3, and 6), and the Golgi marker protein GM130 (blue; enlarged frame a).

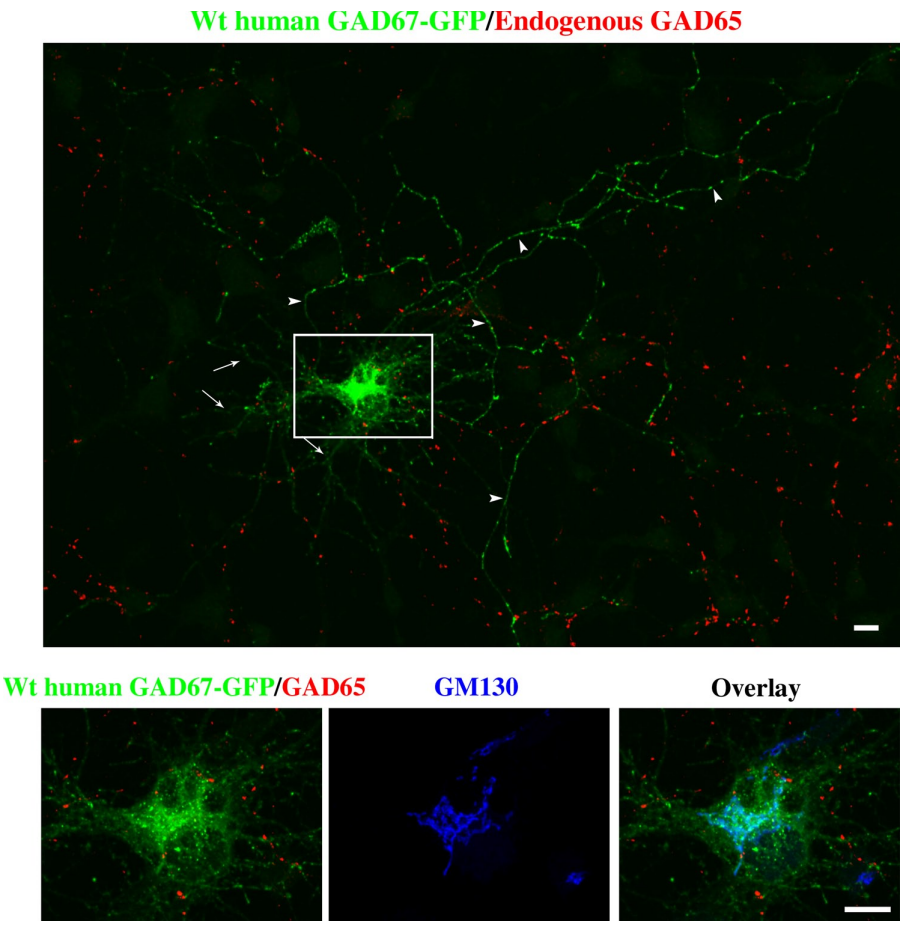

Figure 3. **Human GAD67-GFP is targeted to Golgi membranes, cytosolic vesicles, and presynaptic clusters in hippocampal neurons independent of endogenous GAD65.** Confocal images of a hippocampal neuron singly transfected with wt human GAD67-GFP and triple immunolabeled for GFP (green), endogenous GAD65 (red; MICA 2, 3, and 6 antibodies), and the Golgi marker protein GM130 (blue; enlarged frames from the boxed region shown on the bottom). Wt human GAD67-GFP is not detected in dendrites (arrows) but shows polarized targeting to axonal clusters (arrowheads) and targeting to the Golgi compartment and cytosolic vesicles (enlarged frame) in a neuron devoid of endogenous GAD65 (non-GABAergic neuron). Bars, 10 μm.

proline in this position on the GAD65-independent membrane anchoring mechanism of GAD67, leucine 103 in human GAD67 and leucine 102 in mouse GAD67 were mutated to proline. Confocal analyses of human GAD67(L103P)-GFP and mouse GAD67(L102P)-GFP singly transfected into primary hippocampal neurons revealed that the mutated proteins were diffuse in the soma, dendrites, and axons, and failed to associate with membranes (Fig. 5, B and D), which confirmed the results obtained with rat GAD67(L102P,V473L)-GFP. Quantitative analyses of the presynaptic clustering of wt and mutant human and mouse GAD67-GFP proteins revealed an eight- to ninefold decrease in presynaptic clustering in the human and mouse leucine-to-proline mutants (Fig. 5 E). Thus, the mutation in this position efficiently inhibits the GAD65-independent membrane anchoring mechanism of GAD67 and results in a loss of polarized targeting to axons and presynaptic clustering in the absence of GAD65.

We next asked whether the L102P mutation affects the GAD65-dependent membrane anchoring mechanisms of GAD67. Cotransfection of rat GAD67(L102P, V473L)-GFP with human GAD65-mCherry into hippocampal neurons resulted in targeting of the protein to Golgi membranes, cytosolic vesicles, and presynaptic clusters (Fig. 6). In the presence of human GAD65-mCherry, the mean number of presynaptic clusters containing rat GAD67(L102P, V473L)-GFP was 226.3 ± 10.4 (mean ± SE, $n = 5$), which is 11-fold higher than the mean number of presynaptic clusters for the mutant protein in the absence of GAD65 (20.5 ± 2.8; mean ± SE, $n = 8$; Fig. 6 E).

The number of presynaptic clusters containing rat GAD67(L102P, V473L)-GFP was similar to that for endogenous GAD67 in GABAergic neurons expressing GAD65; singly transfected wt human, rat, or mouse GAD67-GFP in non-GABAergic neurons (see the first paragraph of the Results section); and wt rat GAD65-GFP (Kanaani et al., 2002). Thus, the GAD65-dependent mechanism for membrane anchoring of GAD67 is unaffected by the L102P mutation. The results suggest that each of the two mechanisms can separately mediate targeting of

The transfected neuron is a non-GABAergic neuron devoid of endogenous GAD65. However, GAD65 is seen in axonal puncta of a neighboring GABAergic neuron. Transfected mouse GAD67-GFP is targeted to the Golgi compartment (enlarged frame a), vesicles in the soma (small arrowheads, enlarged frame in A), and axonal puncta (large arrowheads in A) in the absence of endogenous GAD65. (B) Confocal images of presynaptic clusters of a rat hippocampal neuron transfected with mouse GAD67-GFP. Cells were triple immunolabeled for GFP (green), endogenous GAD65 (GAD6 antibody, blue), and synaptophysin (red). The field of view shows the cell body of a non-GABAergic neuron (arrow labeled A) and a GABAergic neuron (arrow labeled B). The cell body of the transfected neuron is not in the field of view. Mouse GAD67-GFP colocalizes with synaptophysin in presynaptic clusters (arrowheads, enlarged frame b), which are devoid of GAD65, showing that the transfected neuron is non-GABAergic. Endogenous GAD65 colocalizes with synaptophysin in presynaptic clusters of the nontransfected GABAergic neuron in the same field of view (arrows, enlarged frame b). Bars, 20 μm.

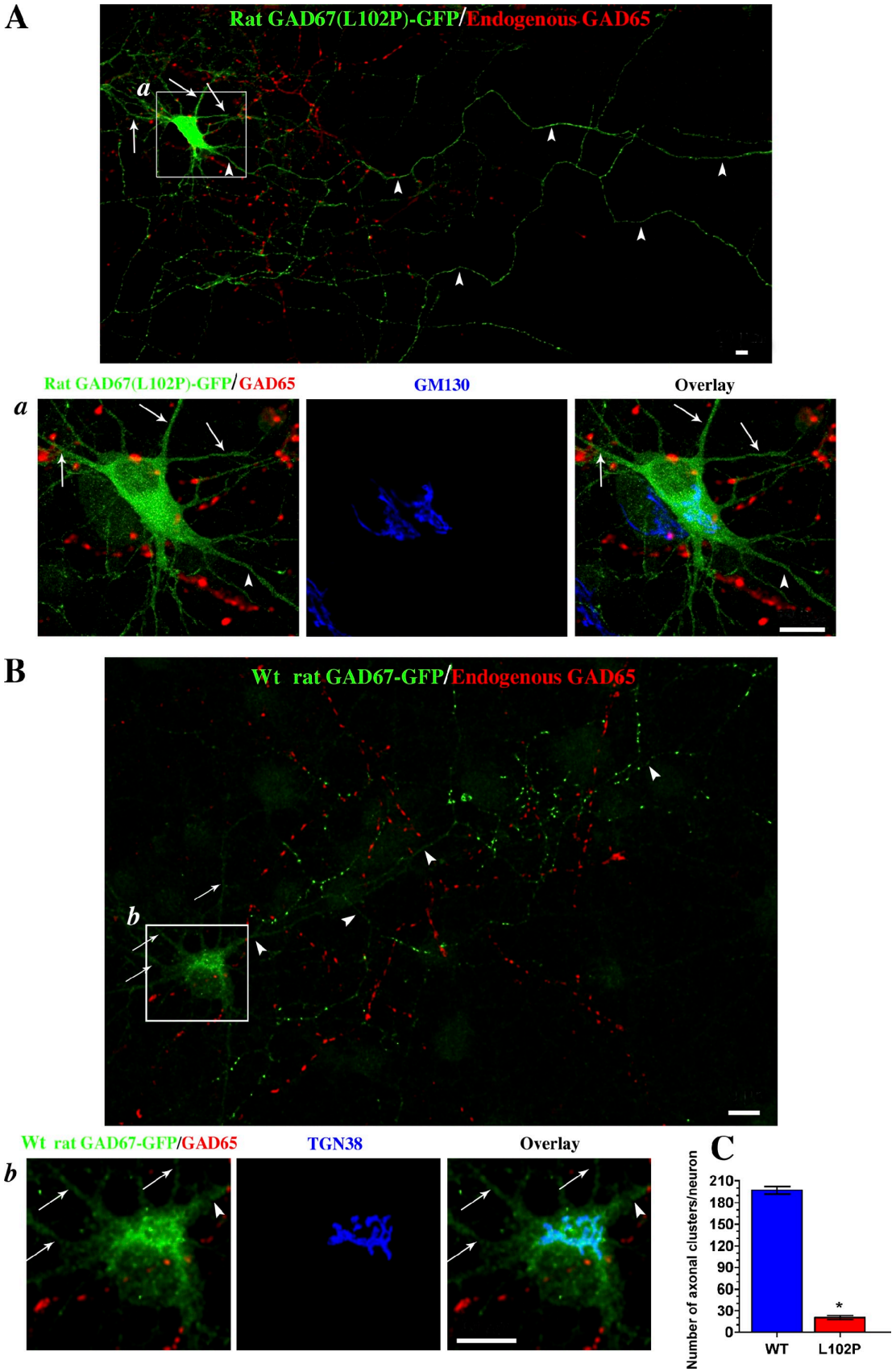

Figure 4. **Reverse mutation restoring leucine in position 102 and valine in position 473 to yield wt rat GAD67 results in anchoring to Golgi membranes and polarized targeting to axonal clusters in hippocampal neurons in the absence of endogenous GAD65.** (A) Confocal images of a hippocampal neuron singly transfected with rat GAD67(L102P, V473L)-GFP and immunolabeled for GFP (green), endogenous GAD65 (red; MICA 2, 3, and 6 antibodies), and the Golgi marker protein GM130 (blue; enlarged frames of the boxed region). Transfected rat GAD67(L102P, V473L)-GFP shows a diffuse cytosolic,

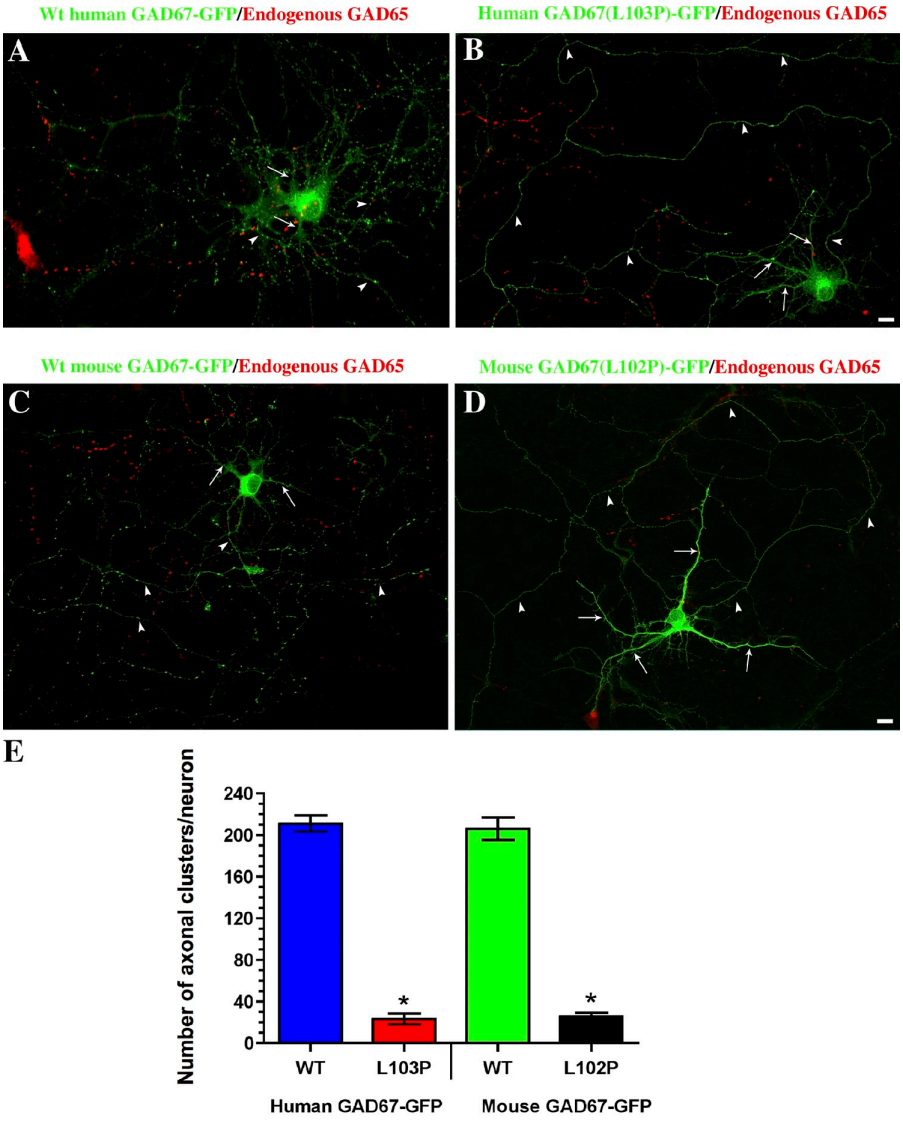

Figure 5. **Mutation of leucine 103 in human GAD67 and leucine 102 in mouse GAD67 to proline abolishes GAD65-independent membrane anchoring of GAD67-GFP in hippocampal neurons.** Projected confocal images of hippocampal neurons singly transfected with either wt human GAD67-GFP (A), human GAD67(L103P)-GFP mutant (B), wt mouse GAD67-GFP (C), or mouse GAD67(L102P)-GFP mutant (D). Neurons were immunolabeled for GFP (green) and endogenous GAD65 (red; MICA 2, 3, and 6 antibodies). Although the wt human as well as mouse proteins are polarized to presynaptic clusters in the axon (arrowheads) of non-GABAergic neurons (A and C), the mutant proteins show a diffuse distribution in the soma, dendrites (arrows), and axon (B and D, arrowheads). Bars, 10 µm. (E) Quantification of the number of presynaptic clusters of the wt and mutant proteins shows an eight- to ninefold decrease in presynaptic clustering of the L103P as well as L102P mutant proteins compared with the wt proteins. Results are presented as mean ± SE (error bars) for 5–7 neurons for each protein. *, $P < 0.0001$.

GAD67 to a similar number of presynaptic clusters and that the presence of both mechanisms in GABAergic neurons expressing both isoforms does not cumulatively increase the number of GAD67-positive presynaptic clusters.

Molecular modeling of the L103P mutation reveals a change in orientation of the N-terminal domain but little effect on the downstream structure of GAD67

The results above show that the fortuitous leucine-to-proline mutation efficiently distinguishes the two mechanisms for membrane anchoring of GAD67 and selectively inhibits the GAD65-independent mechanism while leaving the GAD65-dependent mechanism intact. To assess the potential structural changes induced by the L103P mutation in human GAD67, we used the Protein Data Bank crystal structure (accession no. 2OKJ) of the protein dimer (Fenalti et al., 2007) to computationally model the mutation. In the crystal structure of the human GAD67 dimer, residues 1–92 are lacking in both monomers. However, the segment 93–106 is sufficiently well-defined to regard it as an anchor for the missing segment 1–92. Thus, any change in orientation of the segment 93–106 is likely to produce a significant change in the orientation of the segment 1–92 and thus affect its function. The modeled mutation was performed on

dendritic (arrows), and axonal (arrowheads) localization and fails to associate with Golgi membranes and axonal clusters in a neuron devoid of endogenous GAD65 (non-GABAergic neuron). GAD65 is seen in axonal clusters in a neighboring GABAergic neuron. Bars, 10 µm. (B) Confocal images of a hippocampal neuron singly transfected with rat GAD67-GFP converted to the wt protein (L102, V473) and immunolabeled for GFP (green), endogenous GAD65 (red; MICA 2, 3, and 6 antibodies), and the TGN marker protein TGN38 (blue; enlarged frame b). In contrast to the rat GAD67(L102P, V473L)-GFP mutant, wt rat GAD67-GFP is not detected in dendrites (arrows) but shows polarized targeting to axonal clusters (arrowheads) and targeting to the Golgi compartment (enlarged frame b). Bars, 10 µm. (C) Quantification of the number of presynaptic clustering of wt rat GAD67-GFP and GAD67(L102P, V473L)-GFP in rat hippocampal neurons shows an ~10-fold difference in presynaptic clustering. Results are presented as mean ± SE (error bars) for 5–8 neurons for each protein. *, $P < 0.0001$.

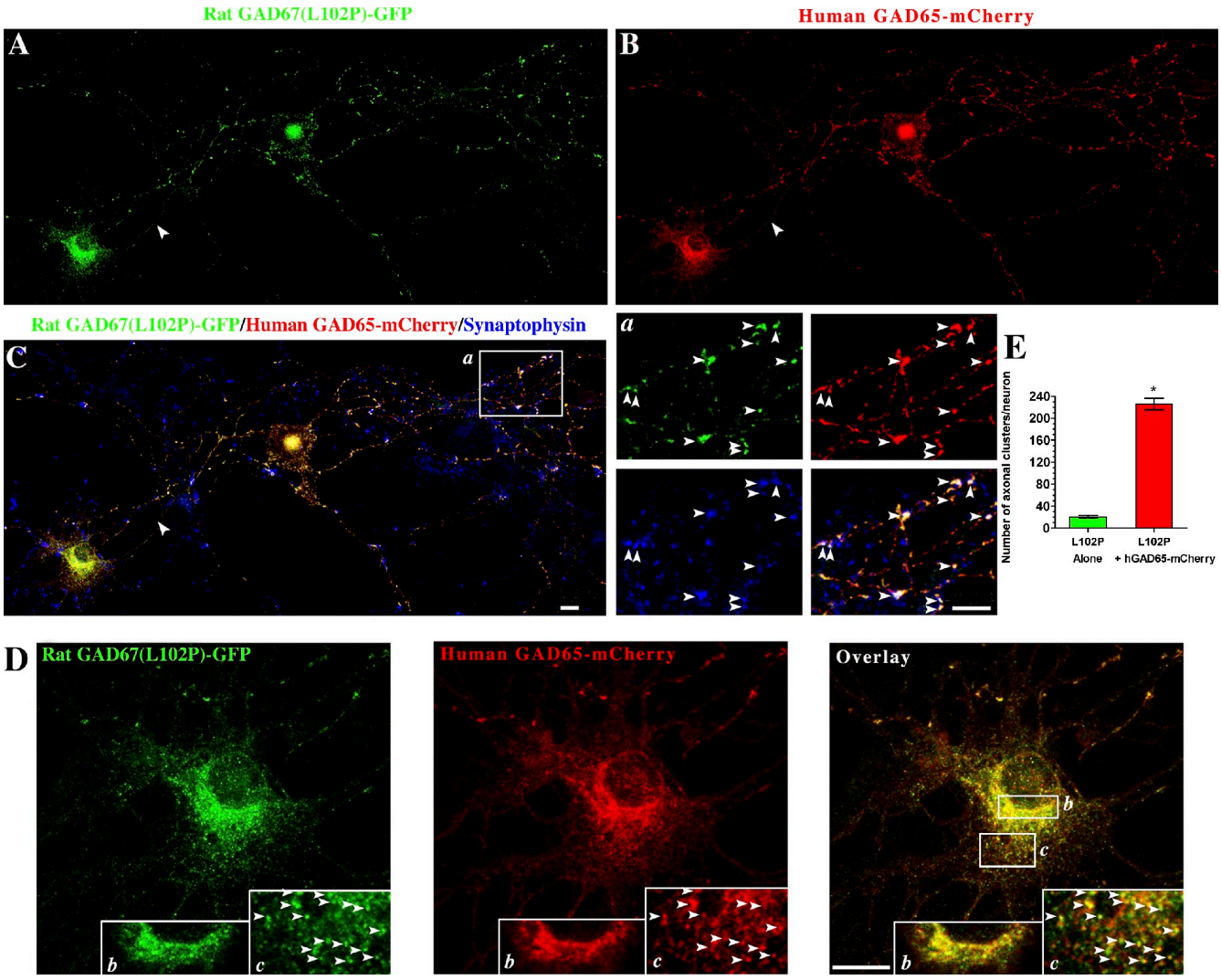

Figure 6. **GAD65 mediates targeting of rat GAD67(L102P, V473L)-GFP to Golgi membranes and cytosolic vesicles, as well as polarized targeting to presynaptic clusters in hippocampal neurons.** Confocal images of a hippocampal neuron cotransfected with rat GAD67-GFP(L102P, V473L)-GFP and human GAD65-mCherry, and triple immunolabeled for GFP (A, green), mCherry (B, red), and synaptophysin (C, blue). In the presence of human GAD65-mCherry, rat GAD67(L102P, V473L)-GFP is targeted to presynaptic clusters, where it colocalizes with human GAD65 and synaptophysin (C, arrowheads in enlarged frame a), Golgi membranes (D, enlarged frame b), and vesicles in the soma (D, arrowheads in enlarged frame c), where it colocalizes with human GAD65-mCherrry. Bars, 10 µm. (E) Quantification of the number of presynaptic clusters in hippocampal neurons expressing rat GAD67(L102P, V473L)-GFP, either alone or with human GAD65-mCherry, shows an 11-fold increase in presynaptic clustering of the cytosolic rat GAD67(L102P, V473L)-GFP when coexpressed with human GAD65-mCherry. Results are presented as mean ± SE (error bars) for eight neurons expressing rat GAD67(L102P, V473L)-GFP and for five neurons coexpressing rat GAD67(L102P, V473L)-GFP and human GAD65-mCherry. *, $P < 0.0001$.

the anchor segment of the A monomer in the form of a reduced model of the crystal structure. This consisted of the six segments a93-a119, a165-a169, b195-b198, b573-b574, b132, and b470, in which the first contains the anchor segment extended by 13 residues to allow for downstream mutation effects and the others represent the local environment with which it directly interacts. As described in the Materials and methods section, this assembly of six segments was subjected to two identical energy refinements under the constraint that residues 116–119 be held fixed. The first refinement was done without the mutation to obtain a control against which measurements could be made that allow for reduced-model effects. In the second refinement, leucine 103 was replaced by a proline. Fig. S2 A shows the crystal structure of the human GAD67 dimer with the segments 93–119 highlighted in each monomer. Fig. S2 B shows the measured change in the position and reorientation of residue 93. It is displaced by 3.5 angstroms; and relative to residue 98, which remains nearly fixed, it undergoes a reorientation of 19.8°. A significant reorientation of the disordered segment 1–92 is therefore expected. Although the molecular modeling results are provisional because of the lack of the 1–92 segment in the crystal structure, they nevertheless suggest a critical role of the conformation of the N-terminal domain, upstream of leucine 103 in human and leucine 102 in rat and mouse GAD67, in the GAD65-independent membrane anchoring of the protein. Conversely, the GAD65-dependent mechanisms for membrane anchoring of GAD67 appear to be unaffected by the changes in the conformation of the N-terminal domain that occur in the leucine-to-proline mutants. This is consistent with the proposed role of heterodimerization of GAD67 and GAD65 in

this mechanism, which does not involve the N-terminal domain (Kanaani et al., 1999) and likely involves the middle and C-terminal domains of GAD67.

The GAD65-independent membrane anchoring machinery for GAD67 is expressed in COS-7, CHO, and MDCK cells

In earlier studies, recombinant rat GAD67 expressed in COS-7 and CHO cells was found to be a soluble molecule (Solimena et al., 1993, 1994; Dirkx et al., 1995), which could only acquire membrane anchoring by dimerization with GAD65 (Dirkx et al., 1995). This is in contrast with the results presented in Figs. 2 and 3 showing that the GAD65-independent mechanism for membrane anchoring and targeting of GAD67 is functional in neurons. We addressed the question of whether the GAD65-independent membrane anchoring machinery for GAD67 is missing in COS-7 and CHO cells. Recombinant wt mouse, rat, or human GAD67 and/or GAD67-GFP were singly transfected into COS-7, CHO, and MDCK cells. Confocal analyses of these experiments showed that human GAD67 (unpublished data) and mouse, rat, and human GAD67-GFP target to Golgi membranes and cytosolic vesicles in COS-7, MDCK, and CHO cells (Fig. S3, A–C; Fig. S4, A, C, and E; and not depicted) similar to what we have shown for GAD65 (Kanaani et al., 2008). Thus, the GAD65-independent membrane anchoring mechanism is present not only in primary neurons but also in COS-7, CHO, and MDCK cells. The earlier studies showing a soluble rat GAD67 in COS-7 and CHO cells in the absence of GAD65 (Solimena et al., 1993, 1994; Dirkx et al., 1995) appear to have used a recombinant rat GAD67 clone derived from the same source as the Bluescript clone, which we have now identified as having the L102P mutation that impairs the GAD65-independent membrane anchoring machinery for GAD67.

The L102/103P mutation effectively distinguishes the GAD65-dependent and -independent membrane anchoring mechanism of GAD67 in COS-7 cells

We analyzed the effect of the L102P or L103P mutation on the GAD65-dependent and -independent mechanism of GAD67 membrane anchoring and subcellular targeting in COS-7 cells. Mouse GAD67(L102P)-GFP, rat GAD67(L102P,V473L)-GFP, and human GAD67(L103P)-GFP were singly transfected into COS-7 cells. In contrast to the wt mouse, rat, and human GAD67-GFP (Fig. S4, A, C, and E), the mutant proteins were diffuse in the cytosol (Fig. S4, B, D, and F). Quantitative analyses of the number of vesicles containing GAD67-GFP per 10 μm^2 showed a 20–30-fold decrease in GAD65-independent vesicular targeting of mouse and rat GAD67(L102P)-GFP and human GAD67(L103P)-GFP, respectively, compared with the wt mouse, rat, and human proteins (Fig. S4 G).

We addressed the possibility that the leucine-to-proline mutation renders GAD67-GFP susceptible to proteolytic cleavage in cells lacking GAD65, such that the observed diffuse staining represents free GFP rather than the GAD67 protein. Rat GAD67(L102P) lacking the GFP tag and GFP-tagged rat GAD67(L102P) were singly transfected into MDCK cells, and immunostained with an antibody to GAD67 or with an antibody to GFP. Confocal analyses revealed a similar diffuse pattern of immunostaining for GAD67(L102P) lacking the GFP tag compared with the GFP tag (unpublished data). Furthermore, SDS-PAGE analyses and immunoblotting of wt and mutant human, mouse, and rat GAD67-GFP proteins expressed in COS-7 cells revealed only the full-length fusion proteins with either the 1701 antibody or an anti-GFP antibody (unpublished data). Thus, the solubility observed for the human, mouse, and rat GAD67 leucine-to-proline mutants is a property of the proteins themselves and not of cleaved GFP.

Cotransfection of the membrane anchoring–deficient rat GAD67(L102P, V473L)-GFP mutant with either rat GAD65 or human GAD65-mCherry resulted in targeting of the protein to Golgi membranes and cytosolic vesicles in COS-7 cells (Fig. S5, B and C). Quantitative analyses revealed that in the presence of rat GAD65 or human GAD65-mCherry, targeting of rat GAD67(L102P, V473L)-GFP to cytosolic vesicles was similar to that of wt human, rat, and mouse GAD67-GFP, and of human GAD65 expressed alone in COS-7 cells (Fig. S5 D). In conclusion and similar to the results in neurons, the L103P mutation in human GAD67 and the L102P mutation in the mouse and rat proteins efficiently inhibit the GAD65-independent mechanism for membrane anchoring and subcellular targeting of GAD67 in COS-7 cells while leaving the GAD65-dependent targeting mechanism intact.

The GAD65-independent membrane anchoring of GAD67 results in distribution of recombinant GAD67 between membrane and soluble fractions in COS-7 cells, which is similar to that of GAD65

Isolation of the GAD65 isoform from brain or from transfected cells reveals a pool of protein with weak membrane affinity, which is easily displaced from membranes, and a pool that is firmly membrane anchored and can only be released from membranes by detergent. The first pool represents nonpalmitoylated GAD65 that cycles on and off ER and Golgi membranes before targeting to TGN after palmitoylation. In subcellular fractionation experiments in COS-7 cells, the hydrophobic but nonpalmitoylated pool of GAD65 is released from membranes during homogenization in 1 mM $MgCl_2$ and a wash of microsomal membrane fractions in 0.5 M NaCl. Approximately 50% of the protein is, however, firmly membrane bound and can only be released from membranes by detergent (Fig. 7; Christgau et al., 1991; Shi et al., 1994). We analyzed the distribution of recombinant mouse and human GAD67 between cytosolic and membrane compartments in COS-7 cells in the absence of GAD65. Cytosol and membrane fractions, washed in high salt, were prepared from singly transfected cells and subjected to SDS-PAGE, followed by Western blotting and immunostaining with the 1701 antibody, which recognizes both GAD65 and GAD67. The rat GAD67(L102P, V473L) variant as well as wt and soluble mutants of GAD65 were analyzed for comparison. The subcellular analyses showed that similar to human GAD65, ~50% of singly transfected wt human and mouse GAD67, respectively, were detected in the washed membrane fractions

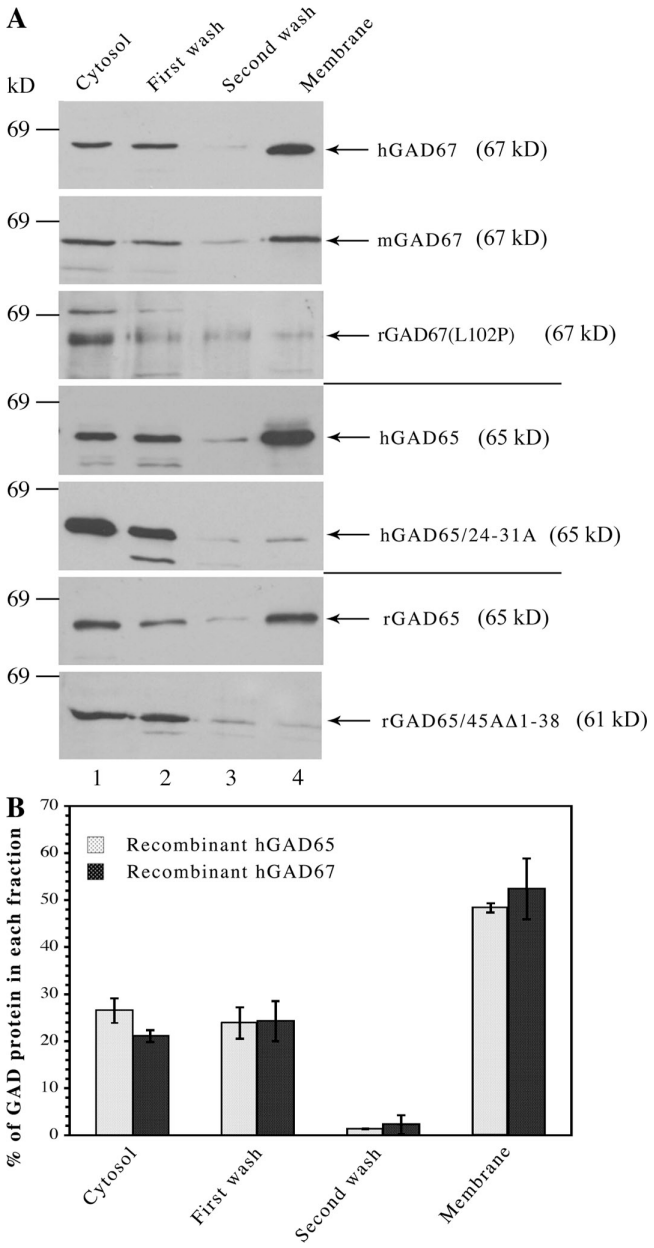

Figure 7. **GAD65-independent membrane anchoring of GAD67 results in distribution of GAD67 between soluble and firmly membrane-anchored pools similar to human GAD65.** (A) Analysis of the subcellular distribution of recombinant GAD67 and GAD65, which lacked a GFP tag expressed in COS-7 cells. COS-7 cells expressing individual GAD67 and GAD65 proteins were subjected to subcellular fractionation. Cytosolic proteins (lane 1), proteins washed from membranes by high salt (lanes 2 and 3), and detergent-extracted membrane proteins (lane 4) were subjected to SDS-PAGE and immunoblotting with the 1701 antibody, which recognizes both GAD65 and GAD67. Recombinant human and mouse GAD67 are primarily detected in the washed membrane fraction similar to human and rat GAD65. Rat GAD67(L102P, V473L), however, is primarily detected in the cytosol fraction similar to the soluble mutants hGAD65/24-31A and rGAD65/45AΔ1-38. Each experiment was performed two to three times with similar results. (B) Quantitative analysis of the subcellular distribution of human GAD65 and GAD67 in COS-7 cells. COS-7 cells expressing human GAD65 or GAD67 were subjected to subcellular fractionation followed by SDS-PAGE and immunoblotting. Quantitation of immunoblots of three independent experiments was performed using NIH Image software. GAD immunoreactivity in each fraction is expressed as the percentage of total GAD. Data are represented as mean value ± SD (error bars). Human GAD67 and GAD65 show similar subcellular distribution in COS-7 cells, with 48.4 ± 1.0% and 52.4 ± 6.5% of hGAD65 and hGAD67, respectively, being firmly membrane bound and only released from membranes by detergent.

(Fig. 7 B and not depicted). Thus, about half of human GAD67 and mouse GAD67 is firmly membrane anchored in COS-7 cells and can only be released from membranes by detergent. In contrast, >90% of the rat GAD67(L102P, V473L) variant is present in the cytosolic fraction, which is similar to the distribution of soluble mutants of human and rat GAD65 (human GAD65/24-31A and rat GAD65/45AΔ1-38, respectively; Fig. 7). Those results suggest that similar to GAD65 (Christgau et al., 1992; Shi et al., 1994; Kanaani et al., 1999, 2002), approximately half of GAD67 has a low membrane avidity and can be released from membranes by a salt wash, whereas the remaining half of the protein is firmly membrane anchored. Thus, the GAD65-independent membrane anchoring mechanism for GAD67 results in membrane association properties similar to those of GAD65 itself.

Discussion

The results presented here reveal that the hydrophilic GAD67 isoform is anchored to membranes and targeted to the Golgi compartment and presynaptic clusters by two different mechanisms. One mechanism, which has been described previously (Dirkx et al., 1995; Kanaani et al., 1999), involves association of GAD67 with the hydrophobic GAD65 isoform in a heterodimeric conformation. The resultant targeting of the GAD67 subunit to membrane compartments is likely mediated by the intrinsic membrane-targeting signals in GAD65. Association with GAD65 is, however, not the sole mechanism for membrane anchoring and targeting of GAD67. Rather, the results shown here reveal that GAD67 possesses an independent capability for membrane anchoring that mediates robust targeting to Golgi membranes, vesicular pathways, axons, and presynaptic clusters. Thus, both GAD65-dependent and GAD65-independent mechanisms mediate targeting of GAD67 to Golgi membranes and polarized localization to axons and presynaptic clusters. We propose that the GAD65-independent mechanism likely involves association with a different protein, a complex of several proteins, or a protein–lipid complex, a postulate based on the demonstration that GAD67 extracted from membrane fractions prepared from the brain of $GAD65^{-/-}$ mice is a hydrophilic molecule devoid of intrinsic hydrophobic moieties (Kanaani et al., 1999). A mutation changing leucine 102 to proline in recombinant rat and mouse GAD67 and the corresponding leucine 103 to proline in human GAD67 abolishes the GAD65-independent mechanisms, and has enabled separate analyses of the two mechanisms.

In the absence of GAD65, the distribution of GAD67 between firmly membrane-bound and weak membrane affinity pools is similar to that of GAD65, which suggests that the membrane anchoring properties achieved by the GAD65-independent method closely mimic those of GAD65 itself. Furthermore, in a separate study, we have shown that polarized targeting of mouse GAD67 to presynaptic clusters in the absence of GAD65 follows an axon-specific Rab5a-dependent trafficking pathway

(unpublished data), first identified for GAD65 (Kanaani et al., 2004). In summation, GAD67 undergoes polarized targeting to axons and reaches its functionally critical location in presynaptic clusters by two distinct mechanisms that each deliver GAD67 to the same subcellular destinations and with similar efficiency: one route is GAD65 independent, whereas the second involves binding to GAD65 to piggyback and exploit its intracellular trafficking.

Targeting domains of GAD67

The GAD65-dependent and -independent mechanisms of membrane anchoring of GAD67 appear to be mediated by distinct domains of GAD67. The GAD65 and GAD67 isoforms self-assemble as nondisulfide linked homodimers via interactions between the middle and C-terminal domains of each monomer, whereas their N-terminal domains are not involved in dimerization (Schwartz et al., 1999; Capitani et al., 2005; Fenalti et al., 2007). The three-dimensional structure of the heterodimer between GAD65 and GAD67 is not available. By analogy with the structure of the GAD65 and GAD67 homodimers (Schwartz et al., 1999; Capitani et al., 2005; Fenalti et al., 2007), and given the high degree of homology between GAD65 and GAD67 in the dimer interfaces, heterodimerization of GAD65 and GAD67 is likely to similarly involve the middle and C-terminal domains of both proteins. As for the N-terminal region, the data presented here suggest that this region of GAD67 is specifically required for the GAD65-independent trafficking and subcellular localization of GAD67. Thus, the L103P mutation in the N-terminal region of human GAD67 and the corresponding L102P mutation in murine GAD67 disrupt the GAD65-independent membrane association, without affecting GAD65-dependent localization, thereby clearly separating the two trafficking mechanisms and associating them with distinct structural domains of the protein. Specifically, the data suggest a critical involvement of the N-terminal region in the GAD65-independent pathway.

GAD67 and GAD65 in Golgi membranes

The Golgi compartment appears to be a depot for newly synthesized GAD65 and GAD67 en route to synaptic clusters. In the case of GAD65, a depalmitoylation step likely performed by one of the acylprotein thioesterases identified in synaptic vesicles (Kim et al., 2008) or in the cytosol (Duncan and Gilman, 1998), releases GAD65 from peripheral membranes and results in its retrograde trafficking back to Golgi membranes by a nonvesicular pathway. Depalmitoylated GAD65 cycles on and off the cytosolic face of Golgi membranes until repalmitoylation by a palmitoyl transferase in Golgi membranes targets it to the TGN, initiating a new cycle of vesicular trafficking to synaptic termini (Kanaani et al., 2008; for review see Baekkeskov and Kanaani, 2009). This dynamic cycling of GAD65 between post-Golgi and Golgi pools demonstrably enables a neuron to rapidly regulate the levels of the enzyme in presynaptic terminals. But does the heterodimerization of GAD67 with GAD65 result in a similar dynamic cycling of the larger isoform between Golgi and post-Golgi membranes? And is there a functional role for both GAD65 and GAD67 in the Golgi compartment? It is unknown whether the transiently active GAD65 is a holoenzyme in both Golgi and presynaptic terminals or whether it is an inactive apoenzyme in Golgi membranes that then becomes activated by infusion of PLP once it has reached a presynaptic location. The constitutively active GAD67, in contrast, likely produces GABA not only on synaptic vesicle membranes, but also on the cytosolic face of Golgi membranes and somatic vesicle membranes. In fact, during development, GABA is generated in the soma by GAD67 and secreted from immature neurons before the maturing of synaptic vesicles (Owens and Kriegstein, 2002a,b), reflecting its roles in shaping of the central nervous system (Wang and Kriegstein, 2009). The cycling of constitutively active GAD67 between presynaptic clusters, where GABA can be rapidly deposited into synaptic vesicles, and the soma, where GABA may either be used as a metabolite and directed to the GABA shunt for energy production (Soghomonian and Martin, 1998) or released by a nonvesicular mechanism, may facilitate dynamic variation in its subcellular localization to variably produce GABA for these distinctive purposes.

A rationale for supplying GAD67 to synaptic vesicles by two distinct mechanisms

Although the GAD65-dependent and -independent mechanisms of membrane anchoring and intracellular trafficking of GAD67 both target the protein to Golgi membranes, vesicular pathways, and presynaptic clusters, they are likely to serve different roles. As depicted in Fig. 8, it is possible that the GAD65-independent trafficking route for delivering GAD67 supplies the constitutive reservoir of glutamic acid decarboxylase (GAD) activity for GABA synthesis. Two distinct functions can, however, be suggested for the GAD65-dependent membrane anchoring of GAD67. First, because GAD65 associates with the vesicular GABA transporter on the cytosolic face of synaptic vesicles (Jin et al., 2003), it is possible that piggybacking of GAD67 enables delivery of GABA synthesized by this isoform to the vesicular GABA-transporter, thereby facilitating a rapid accumulation of GABA in synaptic vesicles. Second, the formation of GAD67-GAD65 heterodimers on synaptic vesicle membranes may serve a role in mediating retrograde transport of GAD67 to Golgi membranes, and thus enable dynamic cycling (and consequent modulation of activity) of this otherwise constitutively activated isoform. This is governed by the depalmitoylation/repalmitoylation cycle that regulates the subcellular distribution of its piggyback transporter GAD65. Thus, GAD65/GAD67 heterodimerization may increase the capacity for GABA synthesis that is regulated by conditional shuttling of the GAD enzymes between the Golgi compartment and synaptic vesicles. As shown in Fig. 8, two distinct GAD67 dimers with different regulatory properties can then reach presynaptic clusters: (1) the constitutively active GAD67 homodimer, which is a stable holoenzyme, provides the basal GABA level, and (2) the GAD65/GAD67 heterodimer, consisting of one subunit of constitutively active GAD67 and one subunit of conditionally active GAD65 (transiently activated by an influx of the coenzyme PLP). A third dimer, the GAD65 homodimer (not shown in Fig. 8), is similarly conditionally regulated by PLP levels. The GAD65 homo- and GAD65/GAD67 heterodimers can cycle between Golgi and synaptic vesicles and contain conditionally active or inactive GAD65 apoenzyme, thereby providing for a

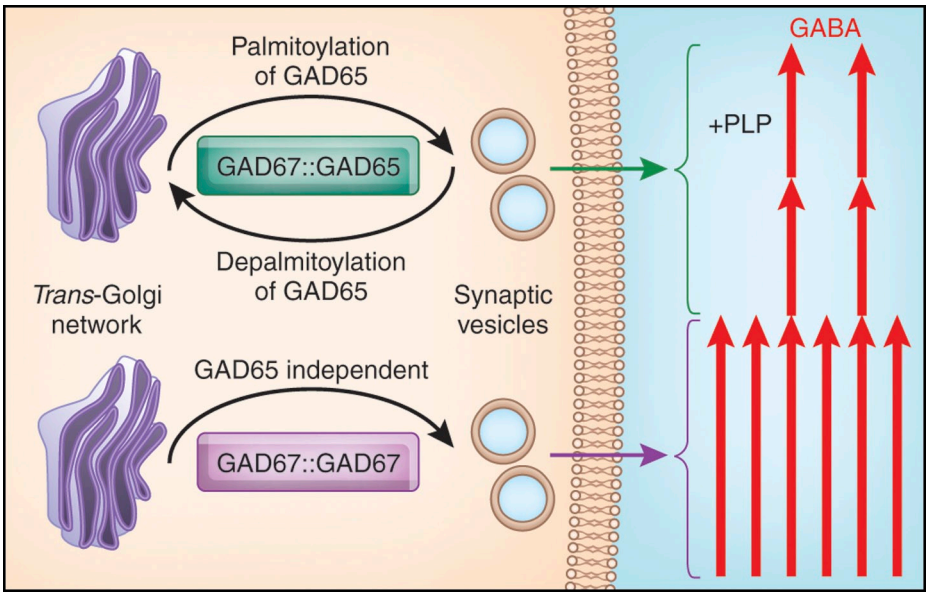

Figure 8. **Schematic model of GABA production.** Homodimers of the constitutively active GAD67 traffic from the TGN to synaptic vesicles via a GAD65-independent mechanism to produce basal levels of GABA. Heterodimers of constitutively active GAD67 and GAD65 (transiently activated by influx of PLP) dynamically cycle back and forth between the TGN and synaptic vesicles, as mediated by the palmitoylation/depalmitoylation cycle of GAD65, to modulate the levels of GABA production and episodically fine-tune GABAergic signaling. Not shown is the GAD65 homodimer, which similarly oscillates between TGN and synaptic vesicles and is dependent on PLP for activation.

means to transiently increase GABA levels so as to fine-tune inhibitory neurotransmission. We envision that the GAD65-independent trafficking of GAD67 serves a distinct and equally important role of producing the core levels of GABA used in synaptic transmission.

Materials and methods

Antibodies

The 1701 rabbit antiserum, which recognizes GAD65 and GAD67 equally well on Western blots (Kim et al., 1993), and a mouse monoclonal antibody to GFP (Covance) were used in immunoblotting and immunofluorescence experiments. The following primary antibodies were used in immunofluorescence experiments: chicken polyclonal antibody raised to purified 6-his–tagged GFP (Millipore); GAD6, a mouse monoclonal antibody specific for GAD65 (Chang and Gottlieb, 1988); a mixture of GAD65-specific human monoclonal antibodies MICA 2, 3, and 6, derived from an islet cell antibody-positive patient (a gift from W. Richter, University of Heidelberg, Heidelberg, Germany; Richter, et al., 1993); K2 rabbit antiserum, which primarily recognizes GAD67 on Western blots (Millipore); mouse monoclonal antibody to the GM130 (BD); mouse monoclonal antibody to the TGN marker protein TGN38 (BD); rabbit polyclonal antibody to synaptophysin (Invitrogen); mouse monoclonal antibody to synaptophysin (Sigma-Aldrich); and Living Colors DsRed rabbit polyclonal antibody raised against DsRed-Express that recognizes mCherry (Takara Bio Inc.). The following secondary antibodies were used in immunofluorescence experiments: Cy3-conjugated AffiniPure donkey anti–mouse, rabbit, or human IgG (Jackson ImmunoResearch Laboratories, Inc.), Alexa Fluor 350 goat anti–mouse IgG, Alexa Fluor 405 goat anti–mouse IgG, Alexa Fluor 488 goat anti–chicken or anti–rabbit IgG, and Alexa Fluor 594 goat anti–rabbit IgG (Invitrogen).

DNA constructs

A 2.4-kb DNA fragment containing the full-length coding region of rat GAD65 was released from a rat GAD65 cDNA clone (provided by A. Tobin, University of California, Los Angeles, Los Angeles, CA) by EcoRI restriction digestion and was inserted into the EcoRI site of the eukaryotic expression vector pMT2 (Invitrogen). A deletion mutant of rat GAD65 lacking aa 1–38 and having the palmitoylation site, cysteine 45, mutated to alanine (rGAD65/45AΔ1-38) in the SV40-based expression vector pSV-SPORT was described previously (Shi et al., 1994). Human GAD65 with aa 24–31 mutated to alanine (hGAD65(24-31A)) was subcloned from Bluescript SK into pSV-SPORT at the EcoRI–NarI sites. Full-length cDNA for human GAD67 in the Bluescript KS vector (a gift from A. Tobin) was subcloned into the pSV-SPORT vector. Full-length cDNA for mouse GAD67 in Bluescript II SK± (a gift from R. Tisch, University of North Carolina at Chapel Hill, Chapel Hill, NC) was subcloned into the SalI site of the pSV-SPORT vector as described previously (Kanaani et al., 1999). The C-terminal fusion proteins of EGFP and mouse or human GAD67 were generated by PCR using mouse or human GAD67 in pSV-SPORT as templates. The PCR products were subcloned into the HindIII and KpnI sites in-frame with EGFP in pEGFP-N3 (Takara Bio Inc.). Full-length rat GAD67 cDNA in Bluescript SK+ (a gift from D. Gottlieb, Washington University, St. Louis, MO; Wyborski, et al., 1990) was subcloned into a pSV-SPORT vector at the EcoRI–HindIII site. The C-terminal fusion protein of EGFP and rat GAD67 was generated by PCR using rat GAD67 in pSV-SPORT as template. The PCR product was subcloned into the HindIII and KpnI sites in-frame with EGFP in pEGFP-N3. Sequencing of the resulting clone rat GAD67-GFP revealed single nucleotide mutations, resulting in a proline instead of leucine in position 102 and a leucine instead of valine in position 473. This construct was renamed rat GAD67(L102P, V473L)-GFP or rat GAD67(L102P)-GFP for short. Both mutations were also present in the original rat GAD67 cDNA in the Bluescript SK+ vector. Targeted mutagenesis to correct the L102P and V473L mutations in the rat GAD67-GFP fusion, and to create a corresponding L103P mutation in the human GAD67-GFP construct and a L102P mutation in the mouse GAD67-GFP construct, was performed using the QuikChange XL Site-Directed Mutagenesis kit (Agilent Technologies). Sequencing was used to confirm the mutated constructs. The construction of the C-terminal fusion protein of EGFP and human GAD65 was described previously (Kanaani et al., 2002). The mammalian expression vector containing mCherry-tagged wt human GAD65 fusion protein (hGAD65-mCherry) was prepared by replacing EGFP with mCherry in hGAD65-EGFP in the pEGFP-N3 mammalian expression vector. The mCherry tag was prepared by PCR amplification using the N-terminal primer containing a BamHI restriction site and the C-terminal primer containing a NotI restriction site, and using pRSETB-mCherry (a gift from R. Tsien, University of California, San Diego, San Diego, CA; Shaner et al., 2004) as a template. The amplification product of mCherry was gel purified, digested with the restriction endonuclease BamHI and NotI, and ligated into a similarly digested pEGFP-N3, which expresses the EGFP fusion protein of GAD65.

Cell culture and transfection

Primary hippocampal neuronal cultures were prepared from embryonic day 18/19 rats according to previously published protocols (Brewer et al., 1993). Hippocampal cultures were transfected at day in vitro 6–7 using

the Effectene lipid-mediated gene transfer kit (QIAGEN). After 2–3 h of incubation at 37°C, the transfection solution was replaced with a 50:50 solution of fresh/conditioned medium. For indirect immunofluorescence analyses, MDCK, COS-7, and CHO-K1 cells were cultured on poly-D-lysine–pretreated glass coverslips in 24-well plates. MDCK cells were maintained in MEM containing Earle's salts and supplemented with 10% fetal calf serum, 25 µM glutamine, and penicillin/streptomycin. COS-7 cells were maintained in DME supplemented with 10% fetal calf serum, 2 mM glutamine, and penicillin/streptomycin. CHO-K1 cells were maintained in F-12K medium supplemented with 10% fetal calf serum, 2 mM glutamine, and penicillin/streptomycin. COS-7 and CHO-K1 cells were transfected using Lipofectamine Plus reagent, and MDCK cells were transfected using Lipofectamine 2000 reagent according to the manufacturer's instructions (Invitrogen). After 5 h of incubation at 37°C, the transfection solution was replaced with fresh culture medium.

Immunofluorescence analyses and quantification

For indirect immunofluorescence, neuronal cultures were fixed for 48–72 h after transfection with either 3.7% PFA in PBS, pH 7.4, for 15 min or in methanol (−20°C) for 10 min (staining for synaptophysin). MDCK cells were fixed 24–48 h after transfection with 3.7% PFA. A chicken polyclonal anti-GFP antibody (Millipore) and a Living Colors DsRed rabbit polyclonal antibody, which was raised against DsRed-Express and recognizes mCherry, were used as primary antibodies to enhance the signal of GFP and mCherry chimeras, respectively, in neuronal and nonneuronal transfections. After fixation, cells were washed with PBS and blocked for 20 min with blocking solution (2% normal goat serum and 0.3% Triton X-100 in PBS). Cells were incubated with primary antibodies in blocking solution for 1 h at room temperature, followed by incubation with the appropriate fluorochrome-conjugated secondary antibodies in blocking solution for 1 h at room temperature. Coverslips were then mounted on slides (Frost Plus; Thermo Fisher Scientific) with Fluoromount-G (Southern-Biotech). Nuclear staining was achieved by mounting the coverslips on slides with a mixture of Fluoromount-G and Vectashield mounting medium with DAPI (Vector Laboratories). Fluorescent images were acquired with either a TCS NT laser scanning confocal microscope (Leica) with a krypton-argon and UV lasers, or TCS SL or TCS SP2 laser scanning confocal microscopes (Leica) equipped with acousto-optical beam splitters and an HCX Plan-Apochromat 63×/1.20 NA oil objective (Leica). Images of 8-bit depth were collected using the Leica confocal software and were prepared for presentation with Photoshop (Adobe). All confocal images represent projections derived from 8–10 consecutive horizontal optical sections estimated at 0.2–0.5 µm in thickness.

For analysis of the number of axonal puncta for mouse and rat GAD67-GFP in rat hippocampal neurons, images were taken at equal exposure times to cover the whole neuronal cell and then were combined using Photoshop. MetaMorph imaging software (Universal Imaging Corp.) was used to determine the number of puncta detected after thresholding the image. The threshold was set to be twice the axonal background. For multichannel imaging, fluorescent dyes were imaged sequentially in frame-interlace mode to eliminate cross talk between the channels. Quantification of the number of mouse, rat, or human GAD67-GFP–containing vesicles in the cytosol of transfected COS-7 cells was performed manually on projected confocal images of COS-7 cells using Openlab software (Perkin-Elmer). The number of vesicles was counted in an area of 50–70 μm^2 and was repeated five times per cell for a total of five cells per condition. The results were expressed as the number of vesicles per 10 μm^2. Results of quantification were analyzed by a *t* test using a two-tailed distribution and two-sample equal variance.

Detergent extraction, subcellular fractionation, and immunoblotting

Detergent extraction with 1% Triton X-114 and subcellular fractionation of COS-7 cells was performed as described previously (Kanaani et al., 1999). Transfected COS-7 cells, grown to 80–90% confluency in a 10-cm plate, were washed twice in ice-cold cell harvesting buffer (20 mM Hepes/NaOH, pH 7.4, 150 mM NaCl, and 10 mM benzamidine/HCl). For detergent extraction, washed cells were incubated on a shaker for 1 h at 4°C in 0.5 ml of hypotonic Hepes buffer (HMAP buffer; 10 mM Hepes/NaOH, pH 7.4, 1 mM $MgCl_2$, 1 mM 2-aminoethylisothiouronium bromide, 0.2 mM PLP, 5 mM EDTA, 0.1 mM *p*-chloromercuriphenyl sulfonic acid, 1 µg/ml leupeptin, 1 mM phenylmethylsulfonyl fluoride, 10 mM benzamidine, 0.1 mM Na_3VO_4, 5 mM NaF, and 5 mM *N*-ethylmaleimide) containing 1% Triton X-114. The lysate was centrifuged at 150,000 *g* for 30 min to remove insoluble debris. For subcellular fractionation, washed cells were homogenized on ice using a glass homogenizer with 0.5 ml of HMAP buffer. The homogenate was centrifuged at 800 *g* for 10 min to remove nuclei and cellular debris. The postnuclear supernatant was centrifuged at 150,000 *g* for 1 h in a TLA 100.3 rotor using a tabletop ultracentrifuge (Beckman Coulter) to separate cytosol and crude membrane fractions. Sedimented membranes were washed twice by resuspension in 0.5 ml of membrane washing buffer (HMAP buffer containing 0.5 M NaCl) and incubation for 1 h, followed by ultracentrifugation at 150,000 *g* for 1 h to pellet the washed membranes. Washed membranes were extracted for 1 h with 0.5 ml of extraction buffer (HMAP buffer containing 150 mM NaCl and 1% Triton X-114) followed by centrifugation for 1 h at 150,000 *g* to separate particulate extract from insoluble debris. For immunoblotting, proteins from each fraction were resolved by SDS-PAGE, transferred to nitrocellulose membranes, and probed with either the 1701 rabbit antiserum and HRP-labeled goat anti–rabbit IgG (Southern-Biotech) or the mouse monoclonal antibody to GFP (Babco) and HRP-labeled sheep anti–mouse IgG (GE Healthcare). Labeled bands were visualized using the ECL plus Western blotting detection system (Ge Healthcare). Blots were quantified using National Institutes of Health Image software (http://rsb.info.nih.gov/nih-image/).

Computational modeling of the L102P mutation

Lacking an atomic level 3D model of mouse or rat GAD67, we used the crystal structure of human GAD67 deposited in the Protein Data Bank (accession no. 2OKJ) to model the mutation by means of energy refinement. In this crystal structure, the leucine 103 residue of human GAD67 is the homologue of leucine 102 in rat and mouse GAD67. Residues 1–92 are missing. Computationally, energy refinement is highly demanding if all the remainder of GAD67 is used as a context of residue 103. Preliminary modeling was therefore devoted to determining the size of the homodimeric segment that begins with residue 93 of monomers A and B, includes residue 103, and can absorb the local change in conformation induced by the replacement of leucine 103 with a proline. In addition, the residues of the local environment with which proline in position 103 would likely interact were determined. Beginning with segment a93–a106, from monomer A and containing the substituted proline, it was refined in isolation under the constraint that its C-terminal residue be held fixed. This constraint serves to model the segment a93–a106 as being attached to the rest of GAD67 and otherwise determine its local interactive environment. Subsequently, the segment a93–a119 was found to be satisfactory and its potential interactive local environment was determined to consist of segments a163–a169 from monomer A and b195–b198, b573–b574, b132, and b470 from monomer B. The assembly of these five environmental segments and segment a93–a119 thus became the object of energy refinement subject to the constraints that residues a116–119 be fixed as well as the backbone of the environmental segments. Fixing backbones permits the side chains to actively interact with the primary segment a93–a119 but otherwise remain fixed and thus represent the rest of GAD67.

The InsightII molecular modeling program (Accelrys, Inc.) was used for the modeling. With AMBER as the force field and a dielectric constant of 10, energy refinement consisted of 3,000 steps of conjugate gradient energy minimization, followed by 5 picoseconds of dynamics, and then a repeat of the same energy minimization. The root mean square energy gradient achieved in both cases of minimization was <0.001. Not using all of GAD67 in our reduced model requires accounting for the isolation of the primary segment 93–119. Refinement of the chosen assembly was therefore first done without mutating the primary segment to give a control against which changes in conformation of the mutated segment could be compared. The mutation was then implemented by replacing leucine 103 in the control segment with a proline and then applying energy refinement to the corresponding assembly. A very important aspect of this subsequent energy refinement is that the first energy minimization application resulted in a conformation that was not too different from that of the control segment, and thus showed that the mutated segment had a locally stable conformation that would probably not result in a significant reorientation of the missing segment 1–92. Applying the 5-picosecond dynamics simulation followed by the energy minimization did, however, result in a much different, locally stable conformation for the mutated segment, which was significantly more stable than the initial one, in that the energy of the mutated assembly was 10% lower than that of the nonmutated one. It is this conformation, with regard to the mutated segment, that is shown in Fig. S2.

Online supplemental material

Fig. S1 shows that the K2 rabbit polyclonal antibody is specific for GAD67, whereas the GAD6 monoclonal antibody is specific for GAD65 in immunofluorescence analyses of rat hippocampal neurons. Fig. S2 shows modeled changes in the structure of the human GAD67 dimer caused by a L103P

mutation. Fig. S3 shows that the GAD65-independent mechanisms of GAD67 membrane anchoring are functional in COS-7, MDCK, and CHO cells. Fig. S4 shows that in COS-7 cells, the leucine-to-proline mutation abolishes targeting of GAD67 to Golgi membranes and cytosolic vesicles in the absence of GAD65. Fig. S5 shows that in COS-7 cells, the GAD65-dependent membrane anchoring of GAD67 is not affected by the L102P mutation. Online supplemental material is available at http://www.jcb.org/cgi/content/full/jcb.200912101/DC1.

We thank Roger Tsien, David Gottlieb, Allan Tobin, Ronald Tisch, and Wiltrud Richter for reagents.

This study was supported by the Nora Eccles Treadwell Foundation and by a National Institutes of Health Diabetes Education and Research Center grant (P30 DK063720) Microscopy Core.

Submitted: 16 December 2009
Accepted: 3 August 2010

References

Asada, H., Y. Kawamura, K. Maruyama, H. Kume, R. Ding, F.Y. Ji, N. Kanbara, H. Kuzume, M. Sanbo, T. Yagi, and K. Obata. 1996. Mice lacking the 65 kDa isoform of glutamic acid decarboxylase (GAD65) maintain normal levels of GAD67 and GABA in their brains but are susceptible to seizures. *Biochem. Biophys. Res. Commun.* 229:891–895. doi:10.1006/bbrc.1996.1898

Asada, H., Y. Kawamura, K. Maruyama, H. Kume, R.G. Ding, N. Kanbara, H. Kuzume, M. Sanbo, T. Yagi, and K. Obata. 1997. Cleft palate and decreased brain gamma-aminobutyric acid in mice lacking the 67-kDa isoform of glutamic acid decarboxylase. *Proc. Natl. Acad. Sci. USA.* 94:6496–6499. doi:10.1073/pnas.94.12.6496

Baekkeskov, S., and J. Kanaani. 2009. Palmitoylation cycles and regulation of protein function (Review). *Mol. Membr. Biol.* 26:42–54. doi:10.1080/09687680802680108

Battaglioli, G.H., H. Liu, and D.L. Martin. 2003. Kinetic differences between the isoforms of glutamate decarboxylase: implications for the regulation of GABA synthesis. *J. Neurochem.* 86:879–887. doi:10.1046/j.1471-4159.2003.01910.x

Brewer, G.J., J.R. Torricelli, E.K. Evege, and P.J. Price. 1993. Optimized survival of hippocampal neurons in B27-supplemented Neurobasal, a new serum-free medium combination. *J. Neurosci. Res.* 35:567–576. doi:10.1002/jnr.490350513

Bu, D.F., M.G. Erlander, B.C. Hitz, N.J. Tillakaratne, D.L. Kaufman, C.B. Wagner-McPherson, G.A. Evans, and A.J. Tobin. 1992. Two human glutamate decarboxylases, 65-kDa GAD and 67-kDa GAD, are each encoded by a single gene. *Proc. Natl. Acad. Sci. USA.* 89:2115–2119. doi:10.1073/pnas.89.6.2115

Capitani, G., D. De Biase, H. Gut, S. Ahmed, and M.G. Grütter. 2005. Structural model of human GAD65: prediction and interpretation of biochemical and immunogenic features. *Proteins.* 59:7–14. doi:10.1002/prot.20372

Chang, Y.C., and D.I. Gottlieb. 1988. Characterization of the proteins purified with monoclonal antibodies to glutamic acid decarboxylase. *J. Neurosci.* 8:2123–2130.

Chattopadhyaya, B., G. Di Cristo, C.Z. Wu, G. Knott, S. Kuhlman, Y. Fu, R.D. Palmiter, and Z.J. Huang. 2007. GAD67-mediated GABA synthesis and signaling regulate inhibitory synaptic innervation in the visual cortex. *Neuron.* 54:889–903. doi:10.1016/j.neuron.2007.05.015

Christgau, S., H. Schierbeck, H.J. Aanstoot, L. Aagaard, K. Begley, H. Kofod, K. Hejnaes, and S. Baekkeskov. 1991. Pancreatic β cells express two autoantigenic forms of glutamic acid decarboxylase, a 65-kDa hydrophilic form and a 64-kDa amphiphilic form which can be both membrane-bound and soluble. *J. Biol. Chem.* 266:21257–21264.

Christgau, S., H.J. Aanstoot, H. Schierbeck, K. Begley, S. Tullin, K. Hejnaes, and S. Baekkeskov. 1992. Membrane anchoring of the autoantigen GAD65 to microvesicles in pancreatic β-cells by palmitoylation in the NH2-terminal domain. *J. Cell Biol.* 118:309–320. doi:10.1083/jcb.118.2.309

Condie, B.G., G. Bain, D.I. Gottlieb, and M.R. Capecchi. 1997. Cleft palate in mice with a targeted mutation in the gamma-aminobutyric acid-producing enzyme glutamic acid decarboxylase 67. *Proc. Natl. Acad. Sci. USA.* 94:11451–11455. doi:10.1073/pnas.94.21.11451

Dirkx, R. Jr., A. Thomas, L. Li, A. Lernmark, R.S. Sherwin, P. De Camilli, and M. Solimena. 1995. Targeting of the 67-kDa isoform of glutamic acid decarboxylase to intracellular organelles is mediated by its interaction with the NH2-terminal region of the 65-kDa isoform of glutamic acid decarboxylase. *J. Biol. Chem.* 270:2241–2246. doi:10.1074/jbc.270.5.2241

Duncan, J.A., and A.G. Gilman. 1998. A cytoplasmic acyl-protein thioesterase that removes palmitate from G protein alpha subunits and p21$^{(RAS)}$. *J. Biol. Chem.* 273:15830–15837. doi:10.1074/jbc.273.25.15830

Fenalti, G., R.H. Law, A.M. Buckle, C. Langendorf, K. Tuck, C.J. Rosado, N.G. Faux, K. Mahmood, C.S. Hampe, J.P. Banga, et al. 2007. GABA production by glutamic acid decarboxylase is regulated by a dynamic catalytic loop. *Nat. Struct. Mol. Biol.* 14:280–286. doi:10.1038/nsmb1228

Hensch, T.K., M. Fagiolini, N. Mataga, M.P. Stryker, S. Baekkeskov, and S.F. Kash. 1998. Local GABA circuit control of experience-dependent plasticity in developing visual cortex. *Science.* 282:1504–1508. doi:10.1126/science.282.5393.1504

Jin, H., H. Wu, G. Osterhaus, J. Wei, K. Davis, D. Sha, E. Floor, C.C. Hsu, R.D. Kopke, and J.Y. Wu. 2003. Demonstration of functional coupling between gamma-aminobutyric acid (GABA) synthesis and vesicular GABA transport into synaptic vesicles. *Proc. Natl. Acad. Sci. USA.* 100:4293–4298. doi:10.1073/pnas.0730698100

Kanaani, J., D. Lissin, S.F. Kash, and S. Baekkeskov. 1999. The hydrophilic isoform of glutamate decarboxylase, GAD67, is targeted to membranes and nerve terminals independent of dimerization with the hydrophobic membrane-anchored isoform, GAD65. *J. Biol. Chem.* 274:37200–37209. doi:10.1074/jbc.274.52.37200

Kanaani, J., Ael.-D. el-Husseini, A. Aguilera-Moreno, J.M. Diacovo, D.S. Bredt, and S. Baekkeskov. 2002. A combination of three distinct trafficking signals mediates axonal targeting and presynaptic clustering of GAD65. *J. Cell Biol.* 158:1229–1238. doi:10.1083/jcb.200205053

Kanaani, J., M.J. Diacovo, Ael.-D. El-Husseini, D.S. Bredt, and S. Baekkeskov. 2004. Palmitoylation controls trafficking of GAD65 from Golgi membranes to axon-specific endosomes and a Rab5a-dependent pathway to presynaptic clusters. *J. Cell Sci.* 117:2001–2013. doi:10.1242/jcs.01030

Kanaani, J., G. Patterson, F. Schaufele, J. Lippincott-Schwartz, and S. Baekkeskov. 2008. A palmitoylation cycle dynamically regulates partitioning of the GABA-synthesizing enzyme GAD65 between ER-Golgi and post-Golgi membranes. *J. Cell Sci.* 121:437–449. doi:10.1242/jcs.011916

Kash, S.F., R.S. Johnson, L.H. Tecott, J.L. Noebels, R.D. Mayfield, D. Hanahan, and S. Baekkeskov. 1997. Epilepsy in mice deficient in the 65-kDa isoform of glutamic acid decarboxylase. *Proc. Natl. Acad. Sci. USA.* 94:14060–14065. doi:10.1073/pnas.94.25.14060

Kash, S.F., L.H. Tecott, C. Hodge, and S. Baekkeskov. 1999. Increased anxiety and altered responses to anxiolytics in mice deficient in the 65-kDa isoform of glutamic acid decarboxylase. *Proc. Natl. Acad. Sci. USA.* 96:1698–1703. doi:10.1073/pnas.96.4.1698

Kim, J., W. Richter, H.-J. Aanstoot, Y. Shi, Q. Fu, R. Rajotte, G. Warnock, and S. Baekkeskov. 1993. Differential expression of GAD_{65} and GAD_{67} in human, rat, and mouse pancreatic islets. *Diabetes.* 42:1799–1808. doi:10.2337/diabetes.42.12.1799

Kim, S.J., Z. Zhang, C. Sarkar, P.C. Tsai, Y.C. Lee, L. Dye, and A.B. Mukherjee. 2008. Palmitoyl protein thioesterase-1 deficiency impairs synaptic vesicle recycling at nerve terminals, contributing to neuropathology in humans and mice. *J. Clin. Invest.* 118:3075–3086. doi:10.1172/JCI33482

Obata, K., T. Fukuda, S. Konishi, F.Y. Ji, H. Mitoma, and T. Kosaka. 1999. Synaptic localization of the 67,000 mol. wt isoform of glutamate decarboxylase and transmitter function of GABA in the mouse cerebellum lacking the 65,000 mol. wt isoform. *Neuroscience.* 93:1475–1482. doi:10.1016/S0306-4522(99)00274-2

Owens, D.F., and A.R. Kriegstein. 2002a. Developmental neurotransmitters? *Neuron.* 36:989–991. doi:10.1016/S0896-6273(02)01136-4

Owens, D.F., and A.R. Kriegstein. 2002b. Is there more to GABA than synaptic inhibition? *Nat. Rev. Neurosci.* 3:715–727. doi:10.1038/nrn919

Patel, A.B., R.A. de Graaf, D.L. Martin, G. Battaglioli, and K.L. Behar. 2006. Evidence that GAD65 mediates increased GABA synthesis during intense neuronal activity in vivo. *J. Neurochem.* 97:385–396. doi:10.1111/j.1471-4159.2006.03741.x

Richter, W., Y. Shi, and S. Baekkeskov. 1993. Autoreactive epitopes defined by diabetes-associated human monoclonal antibodies are localized in the middle and C-terminal domains of the smaller form of glutamate decarboxylase. *Proc. Natl. Acad. Sci. USA.* 90:2832–2836. doi:10.1073/pnas.90.7.2832

Schwartz, H.L., J.M. Chandonia, S.F. Kash, J. Kanaani, E. Tunnell, A. Domingo, F.E. Cohen, J.P. Banga, A.M. Madec, W. Richter, and S. Baekkeskov. 1999. High-resolution autoreactive epitope mapping and structural modeling of the 65 kDa form of human glutamic acid decarboxylase. *J. Mol. Biol.* 287:983–999. doi:10.1006/jmbi.1999.2655

Shaner, N.C., R.E. Campbell, P.A. Steinbach, B.N.G. Giepmans, A.E. Palmer, and R.Y. Tsien. 2004. Improved monomeric red, orange and yellow fluorescent proteins derived from *Discosoma* sp. red fluorescent protein. *Nat. Biotechnol.* 22:1567–1572. doi:10.1038/nbt1037

Shi, Y., B. Veit, and S. Baekkeskov. 1994. Amino acid residues 24-31 but not palmitoylation of cysteines 30 and 45 are required for membrane anchoring

of glutamic acid decarboxylase, GAD65. *J. Cell Biol.* 124:927–934. doi:10.1083/jcb.124.6.927

Shimura, T., U. Watanabe, Y. Yanagawa, and T. Yamamoto. 2004. Altered taste function in mice deficient in the 65-kDa isoform of glutamate decarboxylase. *Neurosci. Lett.* 356:171–174. doi:10.1016/j.neulet.2003.11.041

Soghomonian, J.J., and D.L. Martin. 1998. Two isoforms of glutamate decarboxylase: why? *Trends Pharmacol. Sci.* 19:500–505. doi:10.1016/S0165-6147(98)01270-X

Solimena, M., D. Aggujaro, C. Muntzel, R. Dirkx, M. Butler, P. De Camilli, and A. Hayday. 1993. Association of GAD-65, but not of GAD-67, with the Golgi complex of transfected Chinese hamster ovary cells mediated by the N-terminal region. *Proc. Natl. Acad. Sci. USA.* 90:3073–3077. doi:10.1073/pnas.90.7.3073

Solimena, M., R. Dirkx Jr., M. Radzynski, O. Mundigl, and P. De Camilli. 1994. A signal located within amino acids 1-27 of GAD65 is required for its targeting to the Golgi complex region. *J. Cell Biol.* 126:331–341. doi:10.1083/jcb.126.2.331

Stork, O., F.Y. Ji, K. Kaneko, S. Stork, Y. Yoshinobu, T. Moriya, S. Shibata, and K. Obata. 2000. Postnatal development of a GABA deficit and disturbance of neural functions in mice lacking GAD65. *Brain Res.* 865:45–58. doi:10.1016/S0006-8993(00)02206-X

Stork, O., H. Yamanaka, S. Stork, N. Kume, and K. Obata. 2003. Altered conditioned fear behavior in glutamate decarboxylase 65 null mutant mice. *Genes Brain Behav.* 2:65–70. doi:10.1034/j.1601-183X.2003.00008.x

Tian, N., C. Petersen, S. Kash, S. Baekkeskov, D. Copenhagen, and R. Nicoll. 1999. The role of the synthetic enzyme GAD65 in the control of neuronal γ-aminobutyric acid release. *Proc. Natl. Acad. Sci. USA.* 96:12911–12916. doi:10.1073/pnas.96.22.12911

Wang, D.D., and A.R. Kriegstein. 2009. Defining the role of GABA in cortical development. *J. Physiol.* 587:1873–1879.

Wyborski, R.J., R.W. Bond, and D.I. Gottlieb. 1990. Characterization of a cDNA coding for rat glutamic acid decarboxylase. *Brain Res. Mol. Brain Res.* 8:193–198. doi:10.1016/0169-328X(90)90016-7